

ANGULAR DEPENDENCE OF THE ${}^6\text{Li}(\pi^+, {}^3\text{He}){}^3\text{He}$ REACTION AT 60 AND 80 MeV

B.J. McPARLAND, E.G. AULD, P. COUVERT¹, G.L. GILES, G. JONES, W. ZIEGLER

Department of Physics, University of British Columbia, Vancouver, B.C., Canada, V6T 1W5

X. ASLANOGLU², G.M. HUBER³, G.J. LOLOS, S.I.H. NAQVI, Z. PAPANDREOU³

Department of Physics and Astronomy, University of Regina, Regina, Saskatchewan, Canada, S4S 0A2

D.R. GILL, D.F. OTTEWELL and P.L. WALDEN

TRIUMF, Vancouver, B.C., Canada, V6T 2A3

Received 3 January 1985

Angular distributions of the differential cross sections for the pionic fission ${}^6\text{Li}(\pi^+, {}^3\text{He}){}^3\text{He}$ have been measured at pion energies of 60 and 80 MeV. The differential cross section is found to decrease monotonically with $\cos^2\theta^*$ and is compared with a theoretical prediction.

Exclusive nuclear (p, π) reactions have been investigated intensively during the past decade, but still remain far from being completely understood. The original promise of using the (p, π) process as a probe of the nuclear wavefunction's high-momentum components has been superseded by the interest generated in determining the nature of the reaction mechanism [1].

For those (p, π) reactions that occur below the free $NN \rightarrow NN\pi$ threshold, the nucleons within the target nucleus act coherently in order to create a pion. The only kinematic requirement for such reactions is that the total center of mass kinetic energy exceed the pion rest mass. For pion production using nuclear projectiles the energy is supplied by a composite of nucleons. Below the free nucleon-nucleon threshold, a coherence of both the bombarding nucleons and of those within the target is needed to produce a pion. Such a "doubly-coherent" requirement would suggest a suppressed cross section. However, data for the ${}^3\text{He}({}^3\text{He},$

$\pi^+){}^6\text{Li}$ and ${}^4\text{He}({}^3\text{He}, \pi^+){}^7\text{Li}$ reactions and their inverses [2-6] at these sub-threshold energies show significant cross sections (of the order of nb/sr).

Germond and Wilkin [7] have presented a semi-phenomenological model from which they calculate the cross sections for these reactions by assuming a ${}^4\text{He}-{}^2\text{H}$ clustering for ${}^6\text{Li}$ and using the measured cross sections of the ${}^3\text{He}(p, \pi^+){}^4\text{He}$ reaction as input. An alternative proposal [8] has also been used to explain the ${}^3\text{He}({}^3\text{He}, \pi^+){}^6\text{Li}$ reaction by assuming that the collision produces a Δ -nucleon-hole state with the pion being produced by the Δ decay.

Recognizing that previous data on the ${}^3\text{He}({}^3\text{He}, \pi^+){}^6\text{Li}$ reaction were characterized by a lack of consistent, detailed measurements of the cross section's angular distribution, we have measured the angular distribution of the time-reversed ${}^6\text{Li}(\pi^+, {}^3\text{He}){}^3\text{He}$ reaction at pion energies of 60 and 80 MeV (or 371 MeV and 411 MeV equivalent ${}^3\text{He}$ energies, respectively).

Fig. 1 shows the experimental arrangement. A 95% enriched ${}^6\text{Li}$ target, with an areal density of 112 mg/cm² and enclosed with mineral oil in a polyethylene bag, was mounted over a 7×7 cm² window on a plas-

¹ Permanent address: DPhN/ME, CEN Saclay, 91191 Gif-sur-Yvette Cedex, France.

² Present address: Department of Physics, Florida State University, Tallahassee, FL 32306, USA.

³ NSERC Summer Student Fellowship recipient.

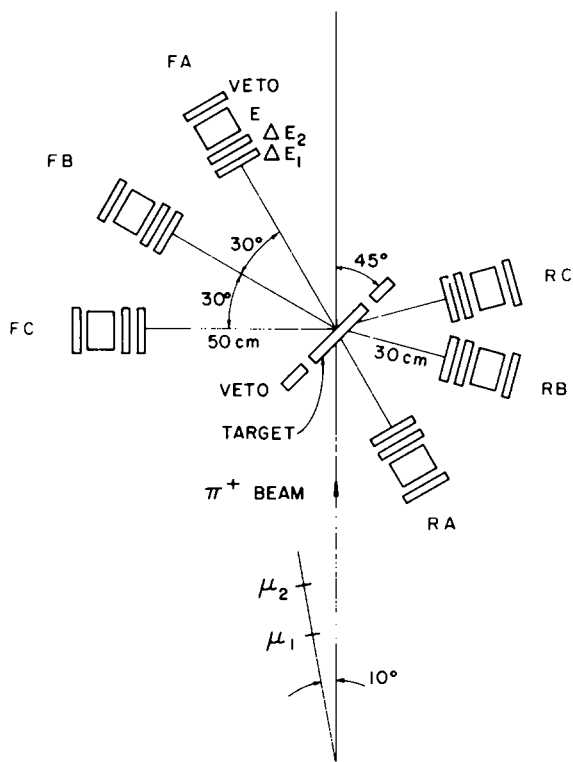


Fig. 1. Diagram of the detection apparatus showing the six arms and the telescopes in the reaction plane. The ($\mu_1 \cdot \mu_2$) counters were mounted at an azimuthal angle of 90° . "A", "B" and "C" refer to the conjugate arms and "F" and "R" refer to "Front" and "Rear".

tic scintillator target holder, which also acted as a veto counter. The reaction products were detected by three pairs of coincident plastic scintillator telescopes with the front arms set at 30° intervals in the lab and 50 cm away from the target and the rear arms at the kinematic conjugate angles and at 30 cm from the target. Each telescope consisted of two ΔE counters ($9 \times 30 \times 0.1$ cm³ each) together with a stopping E counter ($8 \times 30 \times 2.54$ cm³). Behind the E scintillator was a veto counter ($9 \times 30 \times 0.8$ cm³) that served to discriminate against more penetrating background particles, such as pions and protons. Over the kinematic region explored, the maximum range in scintillator of the ^3He nuclei was always less than 1.2 cm. All of the counters in a telescope were coupled to photomultiplier tubes with lucite light guides, except for the ΔE_2 which, due to space restrictions, was coupled to its photomultiplier

tube by a set of flexible fiber-optic cables [9].

The measurements were performed on the M11 pion channel at TRIUMF. The incident pion flux was monitored by detecting decay muons using a coincident pair of thin scintillation counters, mounted at a lab angle of 10° from the beam axis. Two independent calibrations of this telescope were performed using an in-beam counter at the target location and a ^{11}C activation technique [10].

The $\pi^+d \rightarrow 2p$ reaction from a heavy-water target was used to calibrate the pulse heights from the detectors. During this calibration, a hardware-defined event in a conjugate telescope consisted of any two-fold coincidence between pairs of ΔE or E counters, hence permitting the counters' efficiencies to be extracted in the analysis. Although the energy depositions of the protons were significantly different than those of the ^3He nuclei, the associated scintillation light outputs were similar due to the non-linear response of plastic scintillator [11].

For the $^6\text{Li}(\pi^+, ^3\text{He})^3\text{He}$ measurements, an event in a conjugate telescope pair was redefined by requiring a six-fold hardware coincidence in the telescopes (four ΔE 's and two E 's) together with no signals from any of the three veto counters. The data were recorded event-by-event on magnetic tape for off-line analysis.

Solid angles of the telescope pairs were estimated using a Monte Carlo code that incorporated the finite beam size, experimental geometry, reaction kinematics and mean energy losses of the ^3He nuclei. A mean value of about 74 msr was obtained for the lab solid angle. This result was affected by the small fraction of the ^3He nuclei that were stopped prior to reaching the E counters, which led to variations of less than 8% in the solid angle, depending upon the pion energy and detector angle. No explicit corrections for multiple scattering of the ^3He nuclei were made as the estimated effect was less than the uncertainty associated with the solid angle estimation. Only about 2% or less of the ^3He nuclei undergo nuclear reactions while ranging out in the detector. This effect was also not accounted for.

The major systematic errors were due to uncertainties in the beam normalization ($\sim 10\%$), dead-time losses generated by the veto counters ($< 10\%$), and uncertainties in the solid angle estimation ($\sim 5\%$) and in the efficiency measurements ($\sim 3\%$). Summing these in quadrature yielded an overall uncertainty of about 15%.

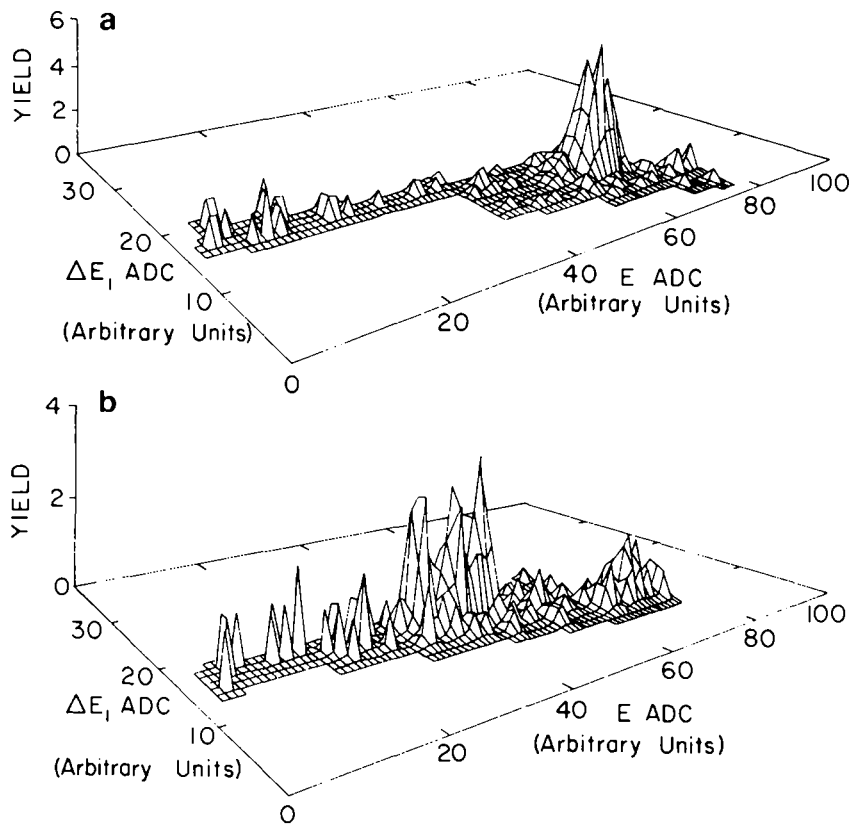


Fig. 2. A characteristic $\Delta E_1 - E$ ADC scatterplot for $T_\pi = 80$ MeV for (a) the front telescope at a lab angle of 30° and (b) the rear telescope at the kinematic conjugate angle. Software cuts have been applied to reject the $Z = 1$ particles.

In the off-line analysis, the proton, deuteron and ^3He spectra were individually identifiable. After the application of software cuts to exclude the background particles in conjugate arms, the ^3He spectra were clearly visible in all telescope pairs. Background runs (with only the polyethylene bag and mineral oil present) were treated identically and the weighted results subtracted from the ^6Li data. No background events survived the strict conjugate software cuts set around the two-body peaks. Examples of three-dimensional conjugate ^3He ADC spectra in a telescope pair are shown in figs. 2a and 2b, where software cuts have been applied to reject the $Z = 1$ particles in both arms.

In figs. 3a and 3b the $d\sigma/d\Omega^*$ of $^6\text{Li}(\pi^+, ^3\text{He})^3\text{He}$ at 60 and 80 MeV are plotted as a function of $\cos^2\theta^*$ and are tabulated in table 1. The errors reflect the counting statistics only. Data from Saclay [3], LAMPF [5] and older measurements made at TRIUMF [6] are also shown in the figures for comparison. A general

observation that can be made of these distributions is the relatively smooth angular structure. The data exhibit an overall consistency, although the LAMPF measurement at 59.3 MeV is over a factor of 2 greater than that expected from our data (a disagreement at the 3σ level). The old TRIUMF data points at 60 and 75 MeV are about a factor of 2 less than our 60 and 80 MeV data, respectively. We are unable to suggest any satisfactory reason for these possible discrepancies other than their being most likely the result of the difficulties inherent in measuring such a low cross section reaction. At each energy, the cross sections measured here decrease monotonically with $\cos^2\theta^*$.

The Germond-Wilkin calculations also shown in figs. 3a and 3b are for the two wavefunction types used in the theory to describe the ^6Li nucleus, a harmonic-oscillator and Woods-Saxon. The calculation for each wavefunction type has an ambiguity due to an uncertainty in the relative signs of two variables used

Table 1
Differential cross sections $d\sigma/d\Omega^*$ (nb/sr).

T_π (MeV)	θ_{LAB} (deg.)					
	15	30	45	60	75	90
60	471.2 ± 50	323.9 ± 38	188.5 ± 30	149.0 ± 25	61.3 ± 17	89.1 ± 20
80	243.4 ± 21	160.3 ± 17	85.7 ± 12	41.0 ± 9	49.1 ± 10	36.6 ± 8

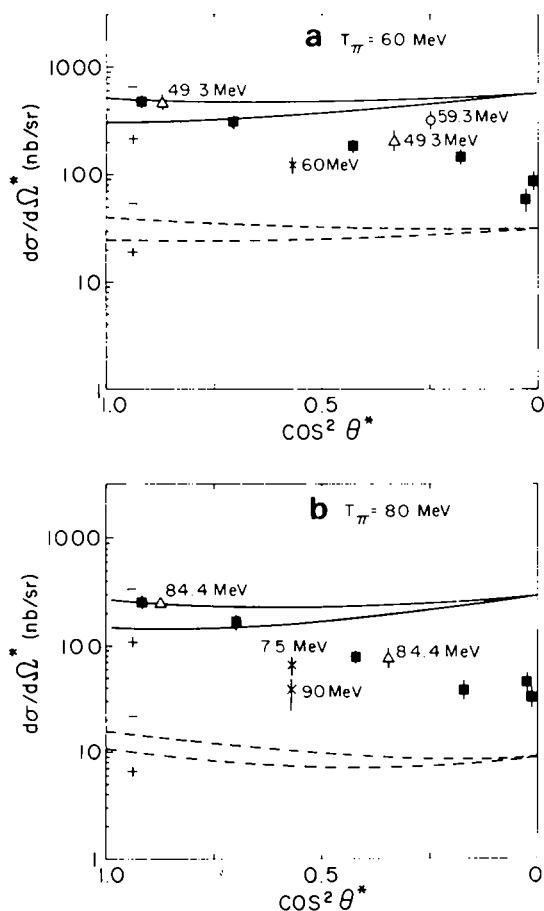


Fig. 3. Differential cross section as a function of $\cos^2\theta^*$ for (a) 60 MeV and (b) 80 MeV pions; the solid squares are from this work, the triangles are from Saclay [3], the circle is from LAMPF [5] and the crosses are old TRIUMF data [6]. The curves represent the Germond–Wilkin calculations using Woods–Saxon (solid line) and harmonic-oscillator (dashed line) wavefunctions. The + and – refer to the relative signs of two variables used in the input data parameterization. Errors shown are statistical only.

by the Germond–Wilkin model to parameterize the ${}^3\text{He}(p, \pi^+){}^4\text{He}$ input data. This ambiguity is reflected by two curves for each calculation. Over most of the range of $\cos^2\theta^*$, the data lies between the two predictions based on the two wavefunction types; at the forward angles ($\cos^2\theta^* > 0.75$), though, the data is well approximated by the Woods–Saxon calculation. However, the observed steep dependence upon $\cos^2\theta^*$ is not predicted by the theory.

The authors would like to acknowledge the assistance of Mrs. D. Sample in the early stages of the data analysis and that of Dr. S. Yen and Messrs. G. Bree and E. Szarmes in the running of the experiment. We would also like to thank Dr. C. Wilkin and Dr. J.-F. Germond for providing us with numerical results from their calculations and for useful discussions. This work was supported in part by the Natural Sciences and Engineering Research Council of Canada.

- [1] H.W. Fearing, Prog. Part. Nucl. Phys. 7 (1981) 113.
- [2] Y. Le Bornec et al., Phys. Rev. Lett. 47 (1981) 1870.
- [3] Y. Le Bornec et al., Phys. Lett. 133B (1983) 149.
- [4] L. Bimbot et al., Phys. Lett. 114B (1982) 311.
- [5] P.D. Barnes et al., Nucl. Phys. A402 (1983) 397.
- [6] G.J. Lolos et al., Phys. Lett. 126B (1983) 20.
- [7] J.-F. Germond and C. Wilkin, Phys. Lett. 106B (1981) 449; J. Phys. G10 (1984) 745.
- [8] K. Klingenberg, M. Dillig and M.G. Huber, Phys. Rev. Lett. 47 (1981) 1654; M.G. Huber and K. Klingenberg, in: Proc. Workshop on Pion production and absorption in nuclei, AIP Conf. Proc., Vol. 79 (AIP, New York, 1981) p. 411.
- [9] M.-J. Yang et al., Nucl. Instrum. Methods 185 (1981) 115; G.M. Huber et al., Nucl. Instrum. Methods 227 (1984) 54.
- [10] B.J. Dropesky et al., Phys. Rev. C20 (1979) 1844.
- [11] T.J. Gooding and H.G. Pugh, Nucl. Instrum. Methods 7 (1960) 189.